

Flow Analysis of an Aircraft that Utilizes Propulsive Aerofoil Technology

J. Haroon Ahmed Khan¹, Maroju Sunanda Rajan², M. Abdul Viger³, K. Maruthupandiyar⁴, D. Govardhan⁵
Research Student¹, Research Student², Research Student³, Associate Professor⁴, Head of the Department⁵,
Department of Aeronautical Engineering, Institute of Aeronautical Engineering, Telangana, India

Abstract: The purpose of our Paper is to explain the Aerodynamic characteristics of an Aircraft that has an Aerofoil Shaped Fuselage. The proposed Aerofoil Shaped Fuselage although has been proven to provide better aerodynamic characteristics than that of the conventional cylindrical shaped fuselage, it also has increased Drag. The Aerofoil shaped fuselage concept, although predominantly used in the 1960's and 1970's has had a steep decline in its usage in commercial and military applications. Our contribution in this field is to propose a NACA 4412 Aerofoil Fuselage Aircraft that has a Swept Back, Mid-Wing configuration with a Twin Tail by designing it in CATIA V5 and then carrying out an analysis of the Model in ANSYS FLUENT 19.2. At various angles of attack, the Lift coefficient and Drag coefficient have been found. The Aerodynamic Characteristic Plots of the Aerofoil Shaped Fuselage Aircraft that have been obtained are Residual Plot, Lift Coefficient Plot, Drag Coefficient Plot, Pressure Plot, Turbulent Kinetic Energy Plot, Velocity Vector Plot for the Complete Continuum, Velocity Vector for the Aircraft and Lift Coefficient/Drag Coefficient vs Angle of Attack Plot has been obtained. Finally, some conclusions have been drawn on the basis of the Computational results of the Design as well as the Literature Survey that has been conducted.

Keyword:- Aerofoil Shaped Fuselage; NACA 4412; ANSYS FLUENT 19.2; Lift Coefficient, Drag Coefficient; Aerodynamic Characteristics; Angle of Attack.

1. INTRODUCTION

Aerofoil Shaped Fuselage can minimise wing drag and structure for different flight regimes, as well as rocket re-entry, whereas a flying wing tries to improve subsonic cruise efficiency by removing non-lifting surfaces. In terms of managing adequate airworthiness, all of these flight conditions provide challenges. They were a significant research topic in the mid-1970s as an attempt to build a compact, lightweight manned aerial vehicle. The US manufactured many airfoil shaped jets as well as multiple launch vehicle that were tested over the Pacific to prove the idea. United States Military abandoned interest in this topic, and extensive research on the Launch Vehicle was halted after it became apparent that the extremely arched airframe would make fuel tankage impractical. In 1957, Dr. Alfred J. Eggers Jr. devised the lifting body idea. Hence, this paper discusses the aerodynamic characteristics of aerofoil shaped fuselage aircraft model that uses a NACA 4412 Aerofoil and recommends ways to reduce the drag, provide a propulsion system suitable for our Model as well as ways to establish the need for research and development to improve the controllability and manoeuvrability of the airplane.

2. METHODOLOGY

NACA 4412 cambered aerofoil has been used for design and investigation of the aerodynamic characteristics of aerofoil shaped fuselage configuration. The Aircraft was designed by using CATIA V5. The results report has been obtained by using Computational Fluid Dynamics (CFD) software, specifically by using ANSYS FLUENT 19.2. The flow of air through the aerofoils is considered to be incompressible and subsonic. The chord length of the aerofoil has been kept 18cm. The Root to Tip length of each Wing is 50cm. The density of air has been considered $\rho = 1.225 \text{ kg/m}^3$. The thickness of the Aerofoil fuselage is 8.2 cm. The total volume of the model is 8250cm³. The free stream airflow has been kept 15 m/sec and the temperature has been considered to be 313K. The design of the model involved attention to detail via trial and error, especially for the fuselage and tail interface. The design analysis was carried out by using a mesh where the size of the element was 5mm with the frequency to be considered as 3. The results converged at 150 iterations. The plots obtained where the Residual Plot, Lift Coefficient Plot, Drag Coefficient Plot, Pressure Plot, Turbulent Kinetic Energy Plot, Velocity Vector Plot for the Complete Continuum, and Velocity Vector for the Aircraft.

Nomenclature	Type
Aerofoil Type	NACA 4412
Chord Length of Aerofoil	180mm
Thickness of Fuselage	200mm
Tip to Tip Length of Both Wing	1200mm
Root to Tip Length of each Wing	500mm

3. LITERATURE REVIEW

Principle

Burnelli was one of several American designers to delve into the idea of the "flying wing." He constructed two aircrafts in the 1920s with massive, Aerofoil-shaped hulls that delivered a significant percentage of the plane's lift.

He believed in the Lift body theory i.e. A lifting body is a type of fixed-wing aeroplane in which the body produces lift. It can indeed be regarded as a fuselage with hardly any traditional wing, in comparison to a flying wing, that is a wing with hardly any traditional fuselage.

Burnelli's findings are supported by the findings of Jahangir et al (2013) as the analysis of the Aerodynamic

Characteristics of an Aerofoil Shaped fuselage did indeed increase the lift of the total aircraft.



Fig. 3.1 Vincent Justus Burnelli's Boeing 754 Model

Advantages

Burnelli's designs used lift-body to get lift from approximately 70 percent of their aero frame weight. The addition of lift from a wide, plain, Aerofoil-shaped fuselage could effectively reduce touchdown speed. On the other hand, Burnelli's planes had very slow final approach speeds. Burnelli's powerful undercarriage would safeguard passengers in the event of a crash, during the 1935 UB-14 catastrophe. Even though the turbines, wings, and elevators were ripped off, the airfoil shaped fuselage remained intact and the crew walked away unhurt. In the case of a traditional aircraft, the wings create lift, and thus account for roughly 15% of the air frames weight, and Jahangir et al (2013) in his research paper has supported this idea in his comparative study of a Cylindrical Shaped fuselage and Aerofoil Shaped fuselage.

Disadvantages

Jahangir et al (2013) claimed that it was difficult to control the aircraft. The papers also concluded that an Aerofoil Shaped fuselage had a comparatively lower L/D ratio with respect to conventional aircraft. In the views of both Pepe (2005) and Rahman et al (2014) the flight testing part for an Aerofoil Shaped Fuselage aircraft was challenging in the context that it had low controllability and manoeuvrability thus requiring a higher skilled pilot to control the aircraft. But as suggested by a NASA aerodynamicist the Burnelli's design would produce induced drag and the skin friction drag would go up because of the large wetted area. Rahman et al (2014), and Jahangir et al (2013) support this idea. One paper discusses aerodynamic characteristics of an Aerofoil Shaped Fuselage and Conventional Cylindrical fuselage. The drag was predominantly more due to Vortex Induced Drag.

Improvements

Pepe's (2005) study provides much relevant information on designing an Aerofoil shaped Aircraft that incorporates a Cross Flow Fan type of propulsion which allowed for a reduced profile drag, this has been supported by Rahman et al (2014) as he said that the design had to be compromised due to the propeller mounting which increased the drag of the Aircraft. Rahman et al (2014) argues convincingly that

using an Aerodynamic Cowling can reduce the profile drag. The L/D ratio could be increased by making structural changes. According to Jahangir et al (2013) and Rahman et al (2014) the fuselage-wing interference effect can be reduced by selecting a High wing type model. There are a few flaws in Jahangir et al's (2013) research paper, firstly a much better prototype model could have been constructed in such a way that it could connect all the pressure tap connections to the multitube manometer for a much better analysis of Pressure Distribution. Secondly, their Analysis in CFD was not highly efficient and accurate as they converged the residuals at 10^{-3} which is not a reliable resolution for analysis. It should be much lower as can be seen in Manish's (2013) analysis where they have converged the residuals at 10^{-6} and have provided the flow over F-16 by using CFD, Solid works and ANSYS Fluent14.



Fig. 3.2 Flying Model of the Boeing 754

4. DESIGNING AND ANALYSIS

Designing the Aircraft in CATIA was done by first, opening the Aerofoil Library and downloading the NACA 4412 Aerofoil. Then we Downloaded Profscan. and opened the .dat file (in Profscan) and saved it in .dxf. then we opened .dxf file in CATIA V5 drawing. Later we opened Part design and pasted the Aerofoil. Then, under the Pad Definition tab of the Workbench, we defined the length of the fuselage and created the Vertical Stabilizer with respect to the XY Plane. On the location we wanted our stabilizer to be, we sketched on the surface and projected it on the body of the airplane. We then created another plane, but this time the Sketch was smaller. A line was created between both the sketches. Multi-Sections Surface was used to create a control surface on the stabilizer.

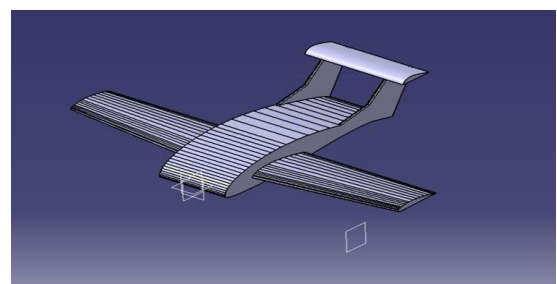


Fig. 4.1 Isometric View of NACA 4412 Aerofoil Fuselage Aircraft

We analysed the Aircraft in Fluent by first opening the Fluent Analysis System then Under Geometry, Import the Geometry from CATIA, Open the Design Modeler and Import the Design File by Clicking Generate. Then, create an Enclosure around the model of 100 mm. Select the entire surface of the model and click on Create and access the Body transformation function, then select Rotate. Under the details of the Rotate box, the axis selection should be for an XY Plane and the angles will be -5, 0, 5, 10 and 15 degrees respectively. Then, Open the Mesh tab and the Element Size is 5mm. Apply the Boundary Conditions by identifying the Velocity Inlet and Outlet on the walls of the Enclosure. Then, Open the Setup tab. Under the Energy Equation-Viscous window, select the conditions that are applicable. In the case of our analysis, it was k-epsilon equation, and enhanced wall treatment. Create the material and Aluminium is considered as the material of the Part. The magnitude of the Velocity is 15 m/s. and the Temperature is 313K. Cross check the boxes for the Residual Plot. and Obtain the report for the design i.e. Facet Maximum which deals with Pressure and Velocity Plots. The frequency is considered to be 3. For the report on Aerodynamic Parameters i.e Drag and Lift, select the Force Report. After all the reports have been uploaded, Initialize the entire flow field. The number of iterations for our analysis is 150. Then, Click on Calculate to generate the results. To obtain the Contours, click on the Contours section, under the Results tab. In a similar manner, Plots have also been obtained, Open the Results tab to see the results of our analysis and Finally, we generated the Report.

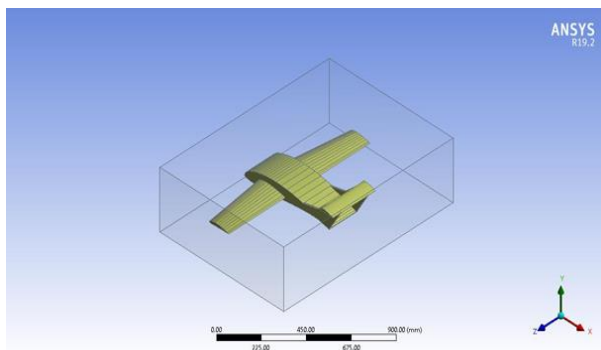


Fig. 4.2 Enclosure around the Model

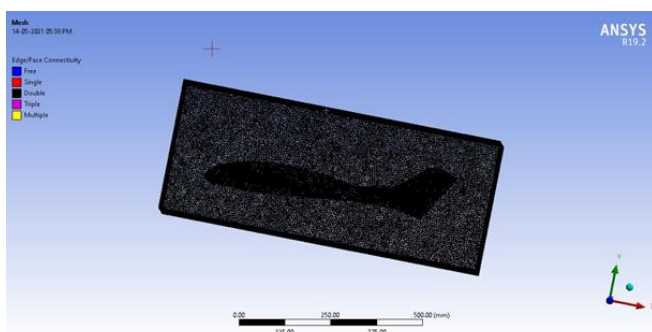


Fig. 4.3 Side-view of the Mesh

5. RESULTS AFTER SIMULATION At -5° Angle of Attack

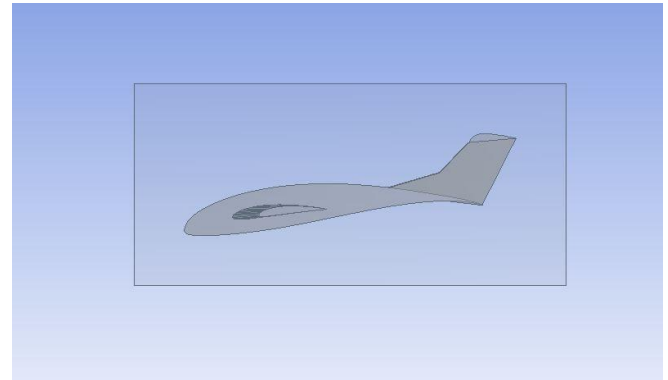


Fig. 5.1 Side View of Model at -5° Angle of Attack

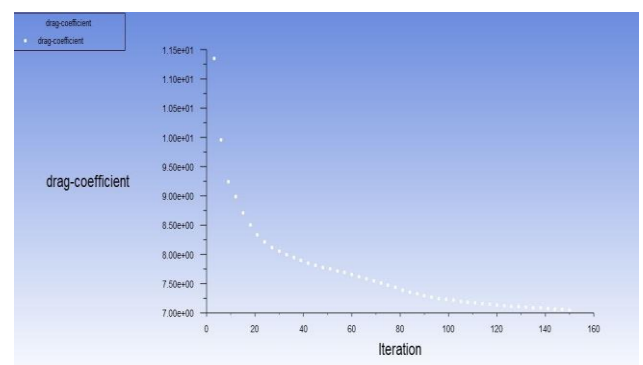


Fig. 5.2 Drag Coefficient Plot at -5° Angle of Attack

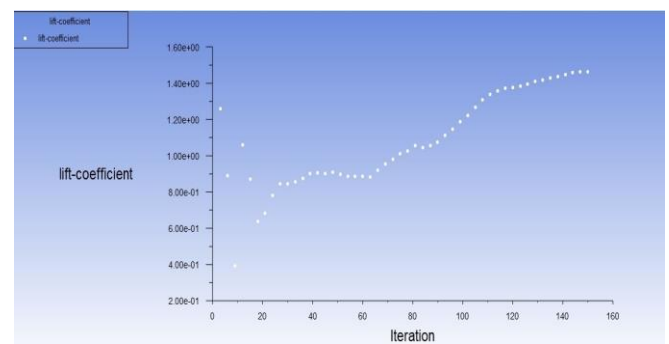


Fig. 5.3 Lift Coefficient Plot at -5° Angle of Attack

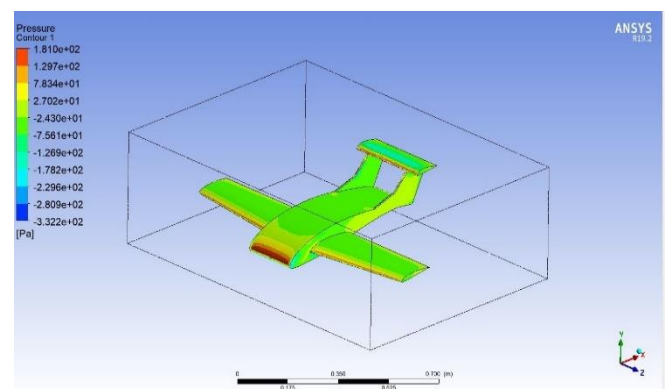


Fig. 5.4 Contours of Static Pressure at -5° Angle of Attack

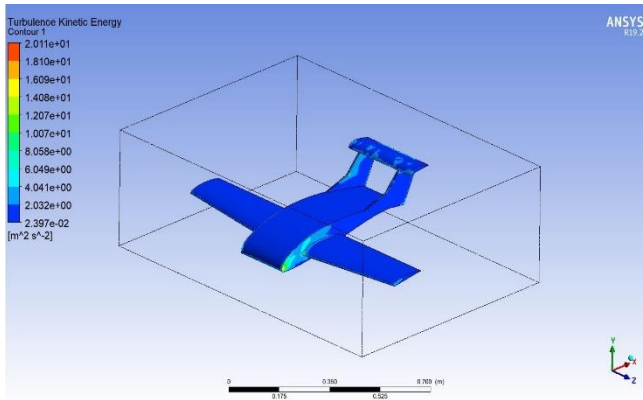


Fig. 5.5 Contours of Turbulent Kinetic Energy at -5° Angle of Attack

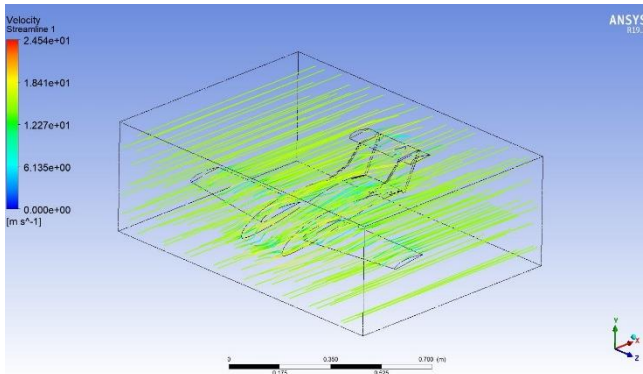


Fig. 5.6 Streamlines of Velocity Vectors over the Model at -5° Angle of Attack

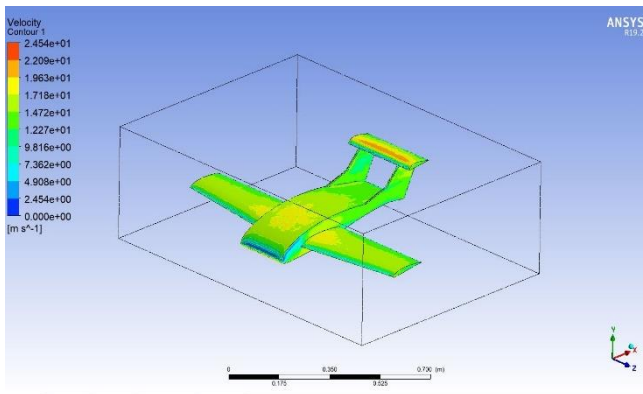


Fig. 5.7 Velocity Contours at -5° Angle of Attack

At 0° Angle of Attack

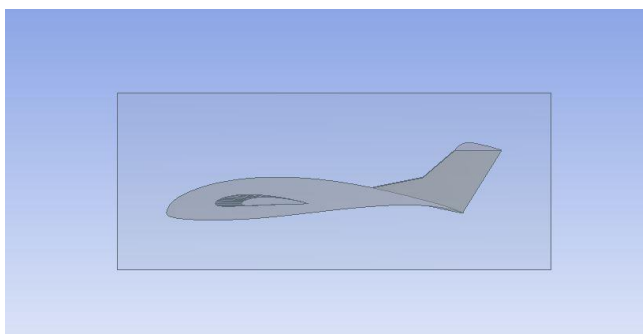


Fig. 5.8 Side View of Model at -0° Angle of Attack

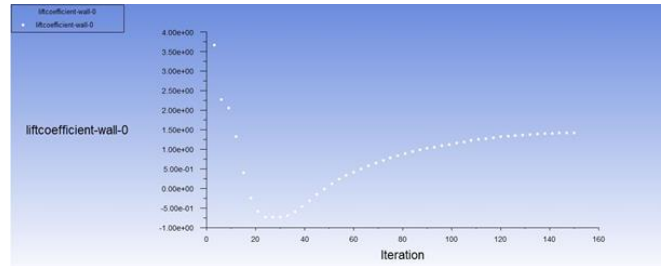


Fig. 5.9 Lift Coefficient Plot

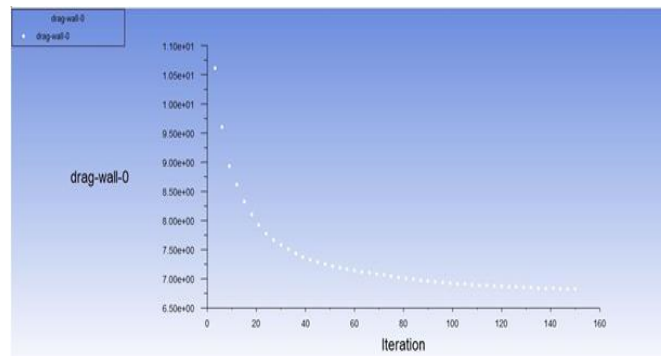


Fig. 5.10 Drag Coefficient Plot

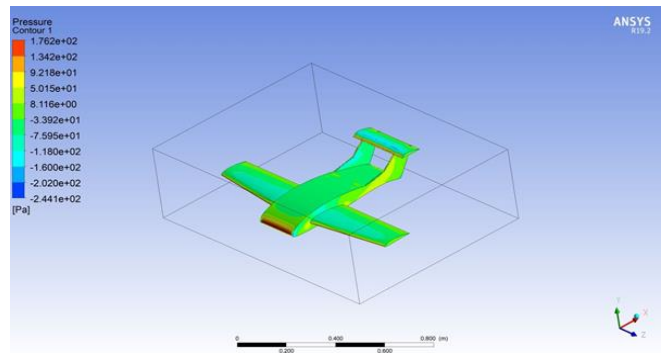


Fig. 5.11 Contours of Static Pressure

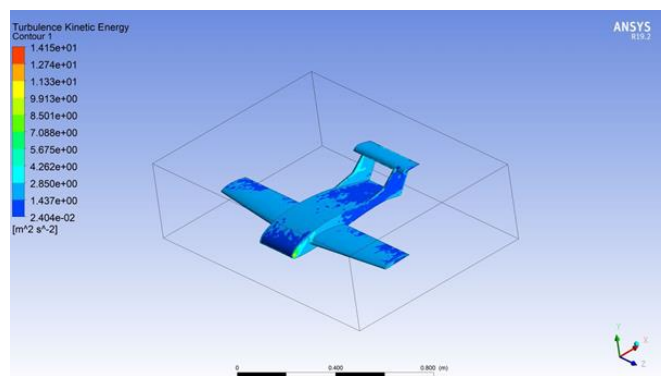


Fig. 5.12 Contours of Turbulent Kinetic Energy

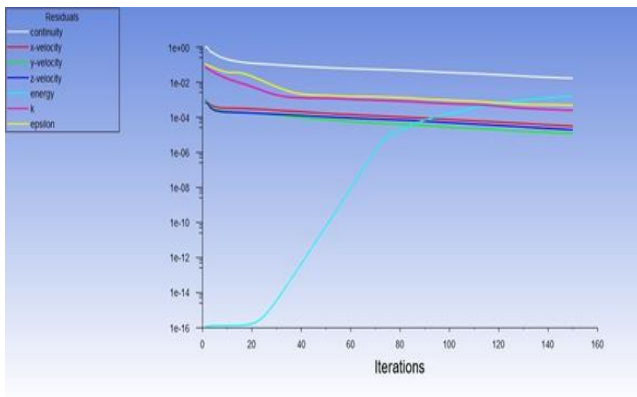


Fig. 5.13 Residual Plot

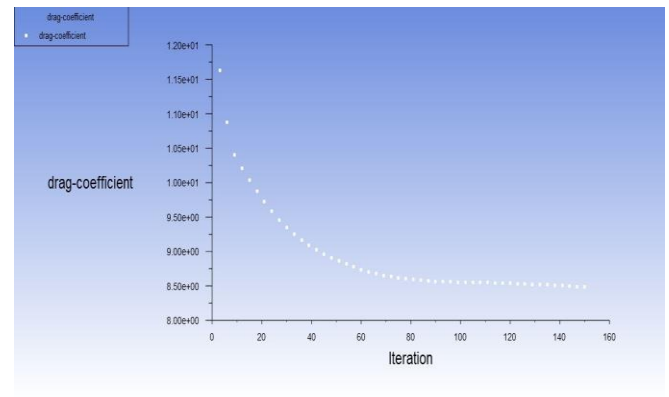


Fig. 5.17 Drag Coefficient Plot at 5° Angle of Attack

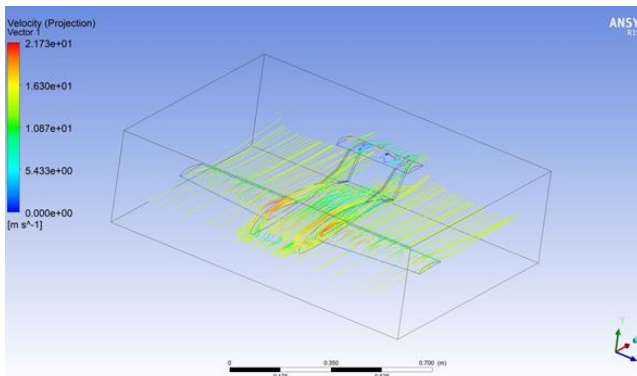


Fig. 5.14 Velocity Contours as they flow over the Model

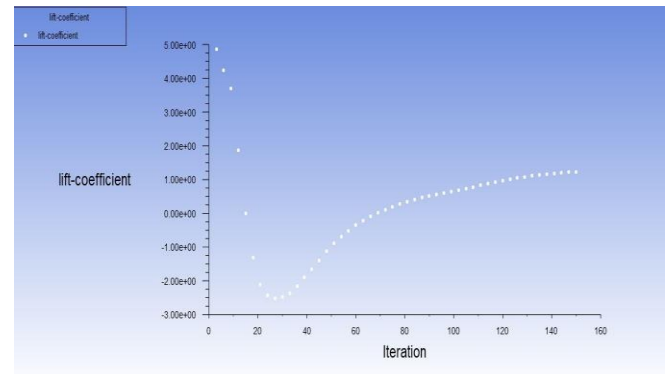


Fig. 5.18 Lift Coefficient Plot at 5° Angle of Attack

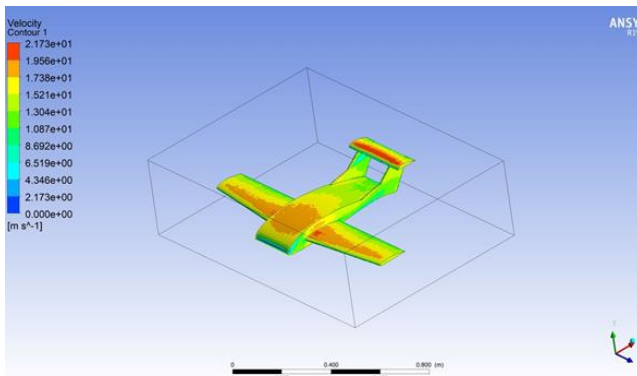


Fig. 5.15 Velocity Vectors for the Model

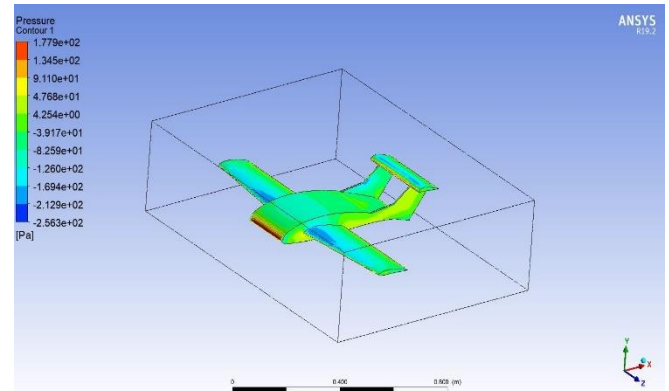


Fig. 5.19 Contours of Static Pressure at 5° Angle of Attack

At 5° Angle of Attack

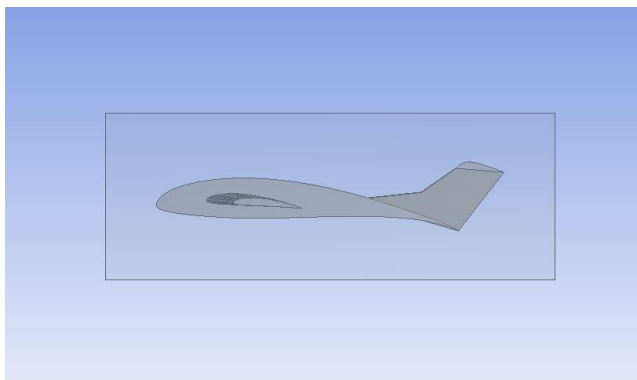


Fig. 5.16 Side View of Model at 5° Angle of Attack

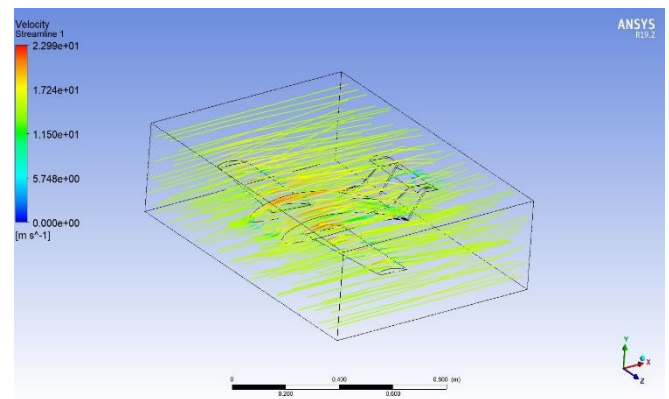


Fig. 5.20 Streamlines of Velocity Vectors over the Model at 5° Angle of Attack

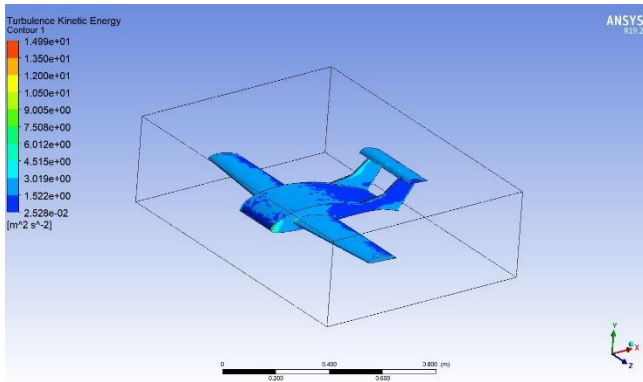


Fig. 5.21 Contours of Turbulent Kinetic Energy at 5° Angle of Attack

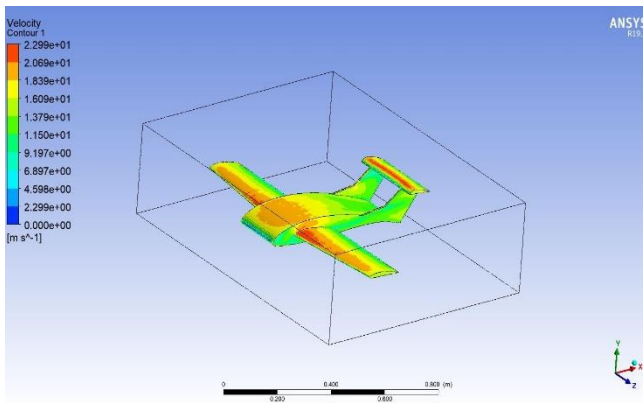


Fig. 5.22 Velocity Contours at 5° Angle of Attack

At 10° Angle of Attack

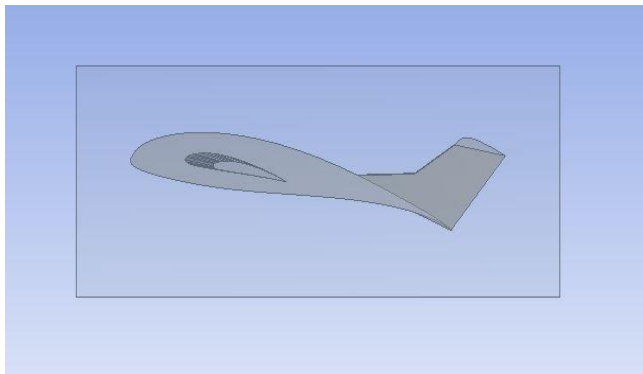


Fig. 5.23 Side View of Model at 10° Angle of Attack

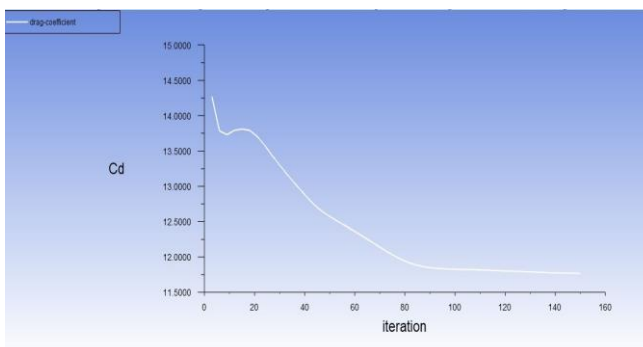


Fig. 5.24 Drag Coefficient Plot at 10° Angle of Attack

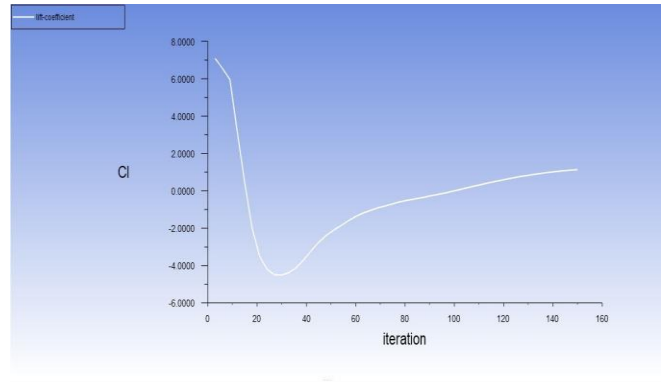


Fig. 5.25 Lift Coefficient Plot at 10° Angle of Attack

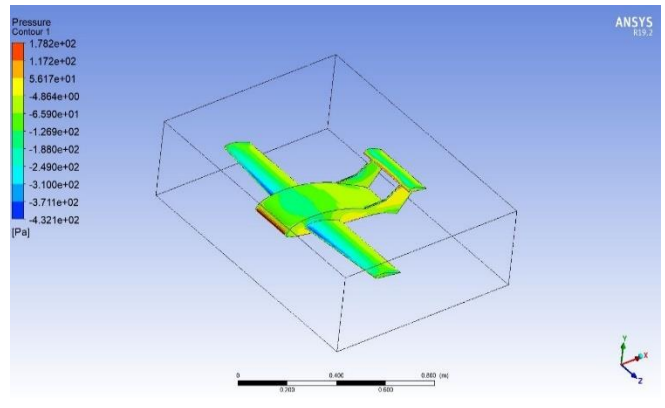


Fig. 5.26 Contours of Static Pressure at 10° Angle of Attack

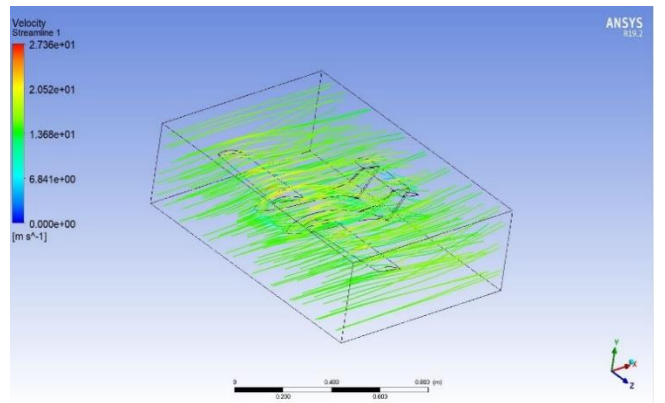


Fig. 5.27 Streamlines of Velocity Vectors over the Model at 10° Angle of Attack

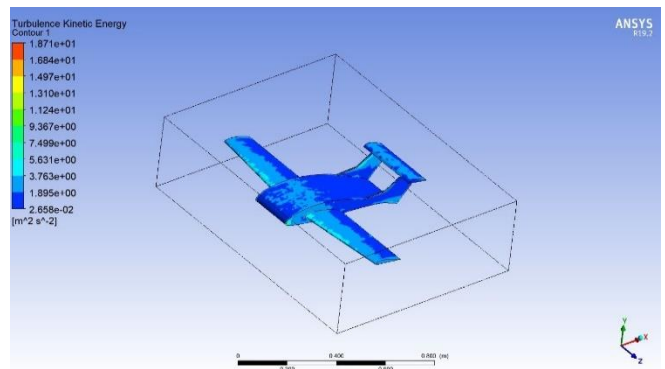


Fig. 5.28 Contours of Turbulent Kinetic Energy at 10° Angle of Attack

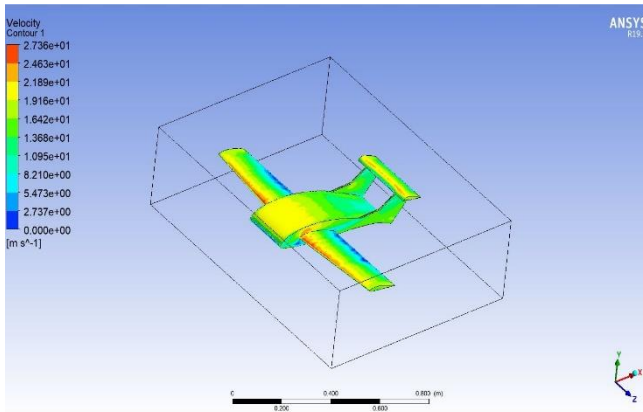


Fig. 5.29 Velocity Contours at 10° Angle of Attack

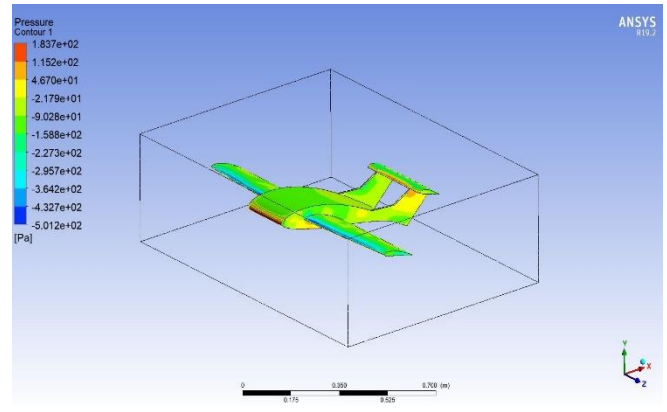


Fig. 5.33 Contours of Static Pressure at 15° Angle of Attack

At 15° Angle of Attack

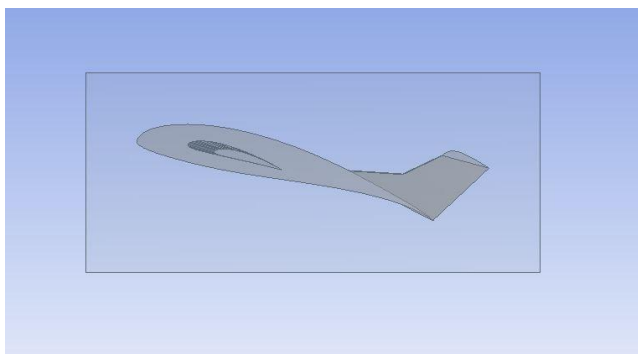


Fig. 5.30 Side View of Model at 15° Angle of Attack

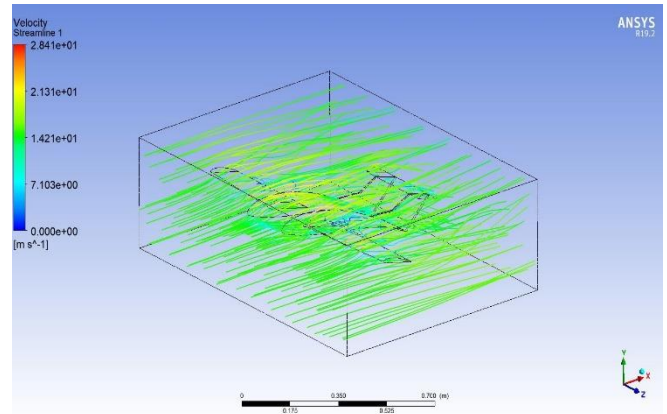


Fig. 5.34 Streamlines of Velocity Vectors over the Model at 15° Angle of Attack

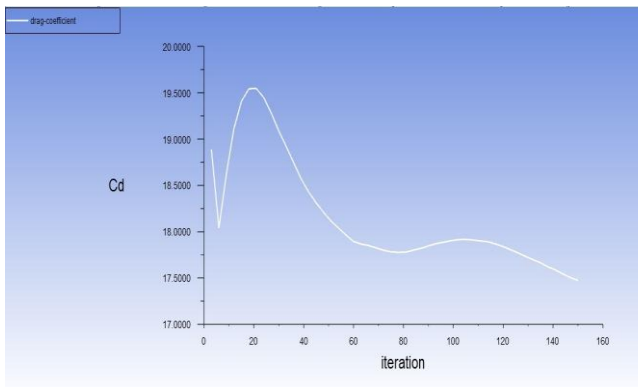


Fig. 5.31 Drag Coefficient Plot at 15° Angle of Attack

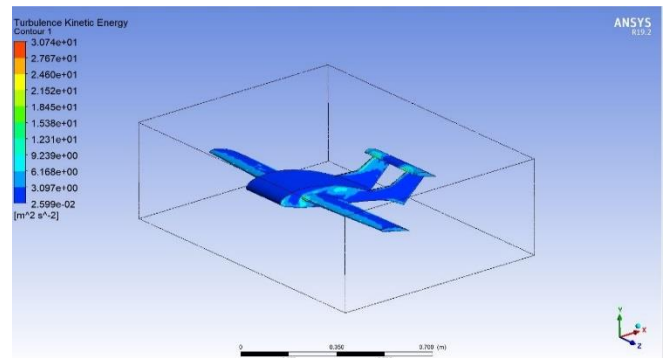


Fig. 5.35 Contours of Turbulent Kinetic Energy at 15° Angle of Attack

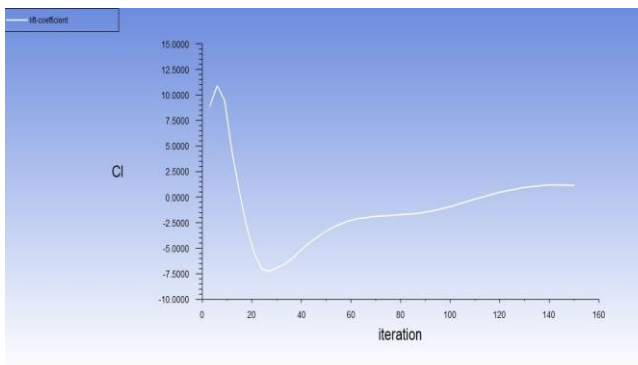


Fig. 5.32 Lift Coefficient Plot at 15° Angle of Attack

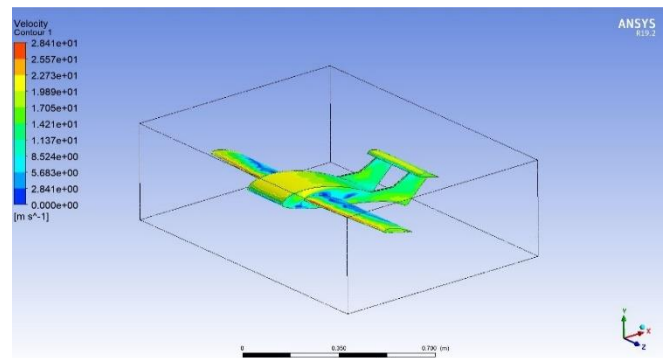


Fig. 5.36 Velocity Contours at 15° Angle of Attack

Cl	Cd	Cl/Cd	Angle of Attack
1.5	11.5	0.13	-5
3.6	10.6	0.34	0
5	11.7	0.43	5
7	14.2	0.49	10
11.5	19.6	0.59	15

Fig. 5.37 Table of Cl, Cd, and Cl/Cd at different Angles of Attacks

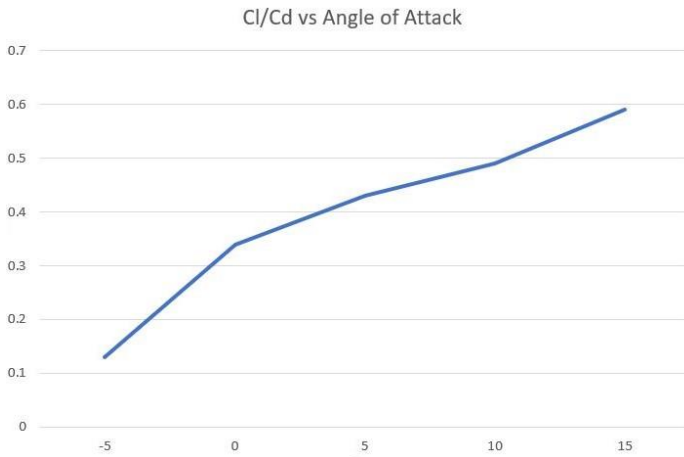


Fig. 5.38 Variation of Cl/Cd with different Angles of Attack

6. DISCUSSION OF RESULTS

The Enclosure around the Model has been created by taking 100mm along positive and negative X, Y and Z axis respectively.

The Maximum Lift Coefficient of the Model at -5° is 1.5 and the Minimum Lift Coefficient to -0.6. From the Drag Coefficient plot it can be seen that the Maximum Drag Coefficient is 11.5 and the Minimum Drag Coefficient is 7. From the Contours of Static Pressure, we can see that the Maximum Pressure is 181 Pa and the Minimum Pressure is -0.03 Pa. It can be seen that at -5° there is a Uniform Magnitude of Low Turbulence Kinetic Energy Contours over the Model. There are no Maximum regions of Turbulent Kinetic Energy over the Upper Surface of the Model. The Velocity Streamlines attain a maximum velocity of 24.5 m/s. In the Velocity Contours Plot, we can see the regions of high velocity and low velocity at -5° Angle of Attack. The Maximum Lift coefficient of the model is seen to be 3.6 after which it reduces to -5 and then remains constant at around 1.6 which is what conventional Aerofoil sections can produce for an Aircraft. From the Drag coefficient plot it can be seen that the drag was initially 11, and then decreased and remained fairly constant at 7. This is coherent from our Literature review that the model has increased drag. The side view of the Mesh has also been shown, wherein each element has a size of 5mm.

From the Contours of Static Pressure, we can see that the Maximum Pressure is 176.2 Pa and the Minimum Pressure is -0.02 Pa. The front portion of the Aerofoil Shaped fuselage as well as the Elevator has a high-pressure region. As has been stated from the Lifting Body Theory, Lift is being generated as there is a low Pressure region across the upper region of the Model.

It can be seen that the Turbulent Kinetic Energy increases as the curvature in the shape of the Model increases. But the Turbulent Kinetic Energy is also at its lowest around the Wing Tips and Trailing Edges of the Wings, this is due to the Lift Induced Drag. From the Residual Plot, it can be seen that the Residuals have converged at 150 iterations. The Velocity Streamlines show that the maximum velocity of 21 m/s is just after the leading edge of the fuselage and the wing. Although there are some regions of low velocity around the Elevator of the Model. By positioning the Elevator above the Fuselage, it avoids the Downwash that is created. In the Velocity Contours Plot, we can see the regions of high velocity and low velocity. As the Air flows from Leading Edge to the Trailing Edge, the Velocity initially increases and then decreases. The average maximum velocity region is over the Elevator of the Model. The Maximum Lift Coefficient of the Model at 5° is 5 and the Minimum Lift Coefficient to -2.5. From the Drag Coefficient plot it can be seen that the Maximum Drag Coefficient is 11.7 and the Minimum Drag Coefficient is 8.5.

From the Contours of Static Pressure, we can see that the Maximum Pressure is 177.9 Pa and the Minimum Pressure is -0.025 Pa.

It can be seen that at 5° there are regions of Low Turbulence Kinetic Energy Contours over the Leading Edge and Trailing Edge of the Fuselage of the Model. There are no Maximum regions of Turbulent Kinetic Energy over the Upper Surface of the Model. The Velocity Streamlines attain a maximum velocity of 22.9 m/s near the Leading Edge of the Model. In the Velocity Contours Plot, we can see the regions of High velocity over the Tail, Wing and Fuselage as well as Low Velocity at 5° Angle of Attack. The Maximum Lift Coefficient of the Model at 10° is 7.6 and the Minimum Lift Coefficient to -5. From the Drag Coefficient plot it can be seen that the Maximum Drag Coefficient is 14.25 and the Minimum Drag Coefficient is 11.75.

From the Contours of Static Pressure, we can see that the Maximum Pressure is 178.2 Pa and the Minimum Pressure is -0.043 Pa.

It can be seen that at 10° there are Low Turbulence Kinetic Energy Contours at the trailing edge of the wing, tail and fuselage of the Model. The Low magnitude of Turbulent Kinetic Energy is not present at the Tips of the Wing and Tail. The Velocity Streamlines attain a maximum velocity of 27.36 m/s. In the Velocity Contours Plot, we can see the regions of high velocity on the front of the Wing and Tail and Low velocity near the Trailing region of the Wing at 10° Angle of Attack. The Maximum Lift Coefficient of the Model at 15° is 11 and the Minimum Lift Coefficient to -7.5. From the Drag Coefficient plot it can be seen that the Maximum Drag Coefficient is 19.5 and the Minimum Drag Coefficient is 17.5.

From the Contours of Static Pressure, we can see that the Maximum Pressure is 183.7 Pa and the Minimum Pressure is -0.05 Pa.

It can be seen that at 15° there are Low Turbulence Kinetic Energy Contours at the trailing edge of the wing, tail and fuselage of the Model. The Low magnitude of Turbulent Kinetic Energy is present over the entire area of the Aerofoil shaped fuselage. The Velocity Streamlines attain a maximum velocity of 28.41 m/s. The flow pattern has also changed considerably as the flow begins to separate. In the Velocity Contours Plot, we can see the regions of Zero Velocity on the Trailing Edge of the Wing thus showing that a region of Stall is formed in the case of 15° Angle of Attack.

From the Cl/Cd vs AOA graph we can see that as the AOA changes from -5° to 15° the value of Cl/Cd also increases.

7. CONCLUSIONS AND FUTURE SCOPE

After Modelling the Aircraft in CATIA V5 and analysing it by using Computational Fluid Dynamics we have obtained various Plots and from our Analysis it can be concluded that our Aircraft Fuselage Model, that incorporates a NACA 4412 Aerofoil, with a Swept back, mid wing Configuration, and Twin Tail Configuration, is Aerodynamically stable and the presence of an Aerofoil Fuselage has generated Increased Lift as well as Increased drag. As the Angle of Attack increases, the Drag also increases considerably and as the angle of attack increased, the Lift Coefficient also increased up to a Maximum point at which Stall takes place i.e. at 15° . The increased drag is due to the induced drag and the skin friction drag because of the large wetted area; the drag was predominantly more due to Vortex Induced Drag.

For Future Readers interested in this Field, we recommend that the Research and Development in the future be focused on decreasing the drag of the Model by making some structural changes such as Winglets and High Wing Configuration as well as making Aerofoil shaped fuselage more Controllable and Manoeuvrable for the Pilot to fly. During the Flight Testing Phase we recommend that Cross Flow Fan technology be used, to reduce the Profile Drag caused by the propulsion system, or else Aerodynamic Cowling for the Propeller mounting can also be used. Further research can be done in a Wind Tunnel to study it's Aerodynamic Characteristics at different angles of attack.

8. REFERENCES

- [1] Jahangir et al, 2013, Alam, G. J., Mamun, M., Ali, M. A. T., Islam, M. Q., & Islam, A. S. (2014). Investigation of the Aerodynamic Characteristics of an Aerofoil Shaped Fuselage UAV Model. *Procedia Engineering*, 90, 225–231
- [2] Jahangir et al, 2013, Alam, G. M. J., & Mamun, M. (2021). Aerodynamic Characteristics of Aerofoil Shaped Fuselage UAV Model and Compare With the Conventional Model Using CFD Software. *Proceedings of the 13th International Conference on Mechanical Engineering (ICME2019)*. Published.
- [3] Manish et al., 2013, Sharma, M., Reddy, R. T., & Priyadarsini, C. I. (2013, May 5). Flow Analysis over an F-16 Aircraft Using Computational Fluid Dynamics.
- [4] Pepe, 2005, Richard L., "Design of a Prototype Model Aircraft Utilizing Propulsive Aerofoil Technology" (2005). Syracuse University Honors Program Capstone Projects. 670.
- [5] The Flying Fuselage, The Boeing 754 Husky, and A Man Named Burnelli – March 2, 2018 | Robert Novell. (2018). Robert Novell.
- [6] Jahangir et al, 2013, Alam, J. C. W. G. M. (2013). Development of design of aerofoil shaped fuselage and cfd investigation of its aerodynamic characteristics | mist international journal of science and technology. *MIST International Journal of Science and Technology*.
- [7] Wikipedia contributors. (2021, April 1). Lifting body. *Wikipedia*
- [8] NASA Armstrong Fact Sheet: Lifting Bodies. (2014). NASA.
- [9] Rahman, I. (2016, August 2). Structural design, analysis and flight test of an unmanned aerial vehicle (uav) having aerofoil shaped fuselage. *MIST Central Library Repository*.